AD-A173 213 IONIC MECHANISMS OF SOOT FORMATION IN FLAMES(U) 1/1
AEROCHEM RESEARCH LABS INC PRINCETON NJ
H F CALCOTE ET AL. MAR 86 AEROCHEM-TP-455
UNCLASSIFIED AFOSR-TR-86-1005 F49620-83-C-0150 F/G 21/1 NL

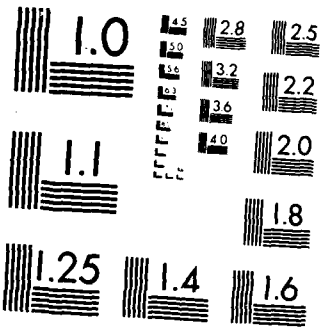

(2)

AeroChem TP-455

AFOSR-TR- 86-1005

AD-A173 213

IONIC MECHANISMS OF SOOT FORMATION IN FLAMES

H.F. Calcote and D.G. Keil
AeroChem Research Laboratories, Inc.
P.O. Box 12
Princeton, New Jersey 08542

March 1986

Approved for public release;
distribution unlimited.

Annual Report for Period 15 September 1983 to 14 September 1984

Approved for Public Release
Distribution Unlimited

Prepared for:
Air Force Office of Scientific Research
Bolling Air Force Base
Washington, DC 20332

UNCLASSIFIED

SECURITY CLASSIFICATION OF THIS PAGE

REPORT DOCUMENTATION PAGE

1a. REPORT SECURITY CLASSIFICATION: Unclassified	1b. RESTRICTIVE MARKINGS: None AD-A173213
2a. SECURITY CLASSIFICATION AUTHORITY	3. DISTRIBUTION/AVAILABILITY OF REPORT: Unlimited
2b. DECLASSIFICATION/DOWNGRADING SCHEDULE	
4. PERFORMING ORGANIZATION REPORT NUMBER(S): TP-455	5. MONITORING ORGANIZATION REPORT NUMBER(S): AFOSR-TR- 86-1005
6a. NAME OF PERFORMING ORGANIZATION: AeroChem Research Laboratories, Inc. / 6b. OFFICE SYMBOL (If applicable)	7a. NAME OF MONITORING ORGANIZATION: Air Force Office of Scientific Research
6c. ADDRESS (City, State and ZIP Code): P.O. Box 12, Princeton, New Jersey 08542	7b. ADDRESS (City, State and ZIP Code): Bolling Air Force Base, DC 20332-6448
8a. NAME OF FUNDING/SPONSORING ORGANIZATION: Air Force Office of Scientific Research / 8b. OFFICE SYMBOL (If applicable): AFOSR/NA	9. PROCUREMENT INSTRUMENT IDENTIFICATION NUMBER: F49620-83-C-0150
8c. ADDRESS (City, State and ZIP Code): Bolling Air Force Base, DC 20332-6448	10. SOURCE OF FUNDING NOS.

PROGRAM ELEMENT NO.	PROJECT NO.	TASK NO.	WORK UNIT NO.
61102F	2308	A2	

11. TITLE (Include Security Classification): Ionic Mechanisms of Soot Formation in Flames

12. PERSONAL AUTHOR(S): H.F. Calcote and D.G. Keil

13a. TYPE OF REPORT	13b. TIME COVERED	14. DATE OF REPORT (Yr., Mo., Day)	15. PAGE COUNT
Annual	FROM 9/15/83 TO 9/14/84	1986 March	29

16. SUPPLEMENTARY NOTATION

17. COSATI CODES			18. SUBJECT TERMS (Continue on reverse if necessary and identify by block number)
FIELD	GROUP	SUB. GR.	
21	01		Soot Formation; Ionic Mechanism; Flame Measurements
21	02		

19. ABSTRACT (Continue on reverse if necessary and identify by block number)

The ionic theory of incipient soot formation has been further evaluated. Accurate temperature profiles through a series of low pressure, 2.7 kPa, acetylene-oxygen flames on either side of the threshold soot index were measured using radiation loss compensated electrically heated thermocouples. With these data and Langmuir probe curves determined in these same flames the absolute ion concentrations were obtained. These were in excellent agreement with similar data obtained by others using a molecular beam ion sampling technique. It was thus demonstrated that the ion concentration peak precedes the appearance of soot, the ion concentration is greater than the concentration of soot particles, and ions decay as soot appears.

Characteristic times were calculated for a $\phi = 3$ flame which indicates that ion molecule reaction rates are sufficient to account for soot formation; they also indicate the

20. DISTRIBUTION/AVAILABILITY OF ABSTRACT	21. ABSTRACT SECURITY CLASSIFICATION
UNCLASSIFIED/UNLIMITED ☑ SAME AS RPT. ☐ DTIC USERS ☐	Unclassified

22a. NAME OF RESPONSIBLE INDIVIDUAL	22b. TELEPHONE NUMBER (Include Area Code)	22c. OFFICE SYMBOL
Julian M. Tishkoff	(202) 767-4935	AFOSR/NA

DD FORM 1473, 83 APR EDITION OF 1 JAN 73 IS OBSOLETE.

UNCLASSIFIED

SECURITY CLASSIFICATION OF THIS PAGE

BLOCK 19 (Continued)

reactions which must be included in any detailed computer model of the process of soot formation--the ultimate goal of this study. Experimental temperature measurements at the soot threshold of flames of varying fuel/oxygen/nitrogen mixtures produced the surprising result that the experimental temperature was a constant for a given fuel although the adiabatic flame temperature varied over a large range.

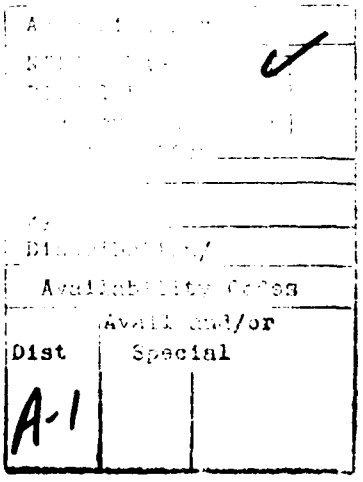

TABLE OF CONTENTS

LIST OF FIGURES

LIST OF FIGURES (Continued)

I. INTRODUCTION

We, at AeroChem, have been protagonists of the theory that chemi-ions play a major role in the soot nucleation process, i.e., in the formation of incipient soot particles from molecular species.[1-5] An understanding of the soot nucleation process represents one of the more significant problems challenging the combustion community today.[6] Numerous laboratories have pursued the problem extensively but to date it remains unresolved. Of all the detailed mechanisms proposed[7] only two remain extant: The free radical mechanism of Frenklach et al.[8] and the ionic mechanism of AeroChem.[2] These are compared in Fig. 1. In order to delineate between the two or to confirm one or the other, or even the simultaneous operation of both, it is necessary to learn something about the nature of the chemical reactions occurring in the initial steps of the soot formation process. This requires a complete description of the detailed composition of the system and its reaction mechanism. Global measurements of soot particles, such as obtained using light scattering techniques, do not provide the type of information required to develop a detailed chemical mechanism from which simple models of the process can be derived. Measurements involving the initial steps are difficult to make and for the most part involve intrusive techniques, especially molecular beam sampling mass spectrometry. Only a few laboratories in the world are equipped to make such measurements; AeroChem is one of them. Thus one of the objectives of this program is to make detailed profile measurements of ion concentrations in the same flames in which Howard and associates at MIT[9-11] have been and are still measuring detailed neutral species profiles. We are also integrating complementary measurements on this same flame by Delfau and associates at Orleans in France[12-14] and Homann and associates at Darmstadt in Germany.[15-18] Our measurements include, in addition to individual ion concentrations by mass spectrometry, the use of Langmuir probes to measure the total ion concentrations, and electrically heated thermocouples to measure temperature profiles. Our use of Langmuir probes in sooting flames represents the first such probe measurement of the concentration of ions of the size of small particles so that considerable time was devoted to diagnostic development. A somewhat similar situation existed for the use of thermocouple probes in sooty flames. To assure that the flames we are studying are exactly comparable to those used by Howard et al. at MIT we have duplicated their burner.

In addition, during this reporting period, we have made some measurements of the effect of temperature on the first appearance of soot in atmospheric flames.

In this report we summarize the results obtained on this program during this 12 month period.

The work statement for this program defines two phases. In Phase I experiments are to be done in well-studied flames of benzene/oxygen and acetylene/oxygen. The measurements include temperature profiles, Langmuir probe curves of total ion concentration, and mass spectrometer profiles of individual ion concentrations. Phase II involves model development of the individual processes involved in incipient soot formation, e.g. study of the rates of ion

and particle formation, rate of production of large molecular ions, the temperature of the growing particle and its affect on thermal ionization, thermal ionization of large molecules, and ion molecule rate coefficients. Considerably more time was consumed in the temperature profile measurements than anticipated, at the expense of other experimental tasks.

II. STATUS OF RESEARCH

The research done during this period which has already been published will be only briefly surveyed here; the work still in progress or as yet unpublished will be presented in more detail.

A. MIT BURNER

The MIT burner was duplicated from designs furnished by Howard.[19] It is constructed of copper and consists of three major pieces. The burner surface is a 7.1 cm diameter, 1.27 cm thick copper plate with about 600 1 mm holes drilled in a hexagonal close-packed pattern such that the center to center distance is 0.254 cm. This plate is press-fit into a thin-walled (0.3 cm thick) support cylinder, which is threaded onto the bottom mixing chamber and water-cooling chamber. Therefore the burner surface is cooled by conduction down the copper support cylinder to the water jacket at the burner base. This burner operates with a surface temperature ($\sim$ 425 $\pm$ 25 K at burner edge) which is greater than our directly cooled stainless steel burner.[20] We had considerable difficulties getting this burner to operate in our system; the flame showed a slow periodic oscillation. We finally traced this problem to a gas mixing chamber and eliminated the difficulty by simply changing the manner in which the two gases were brought into the chamber. No similar problem was observed with our stainless steel burners which have larger pressure drops across the burner.

B. TEMPERATURE MEASUREMENTS

Accurate temperatures are required to interpret the various data to be analyzed and they were not available (to our satisfaction) in the flames in which we were interested. For our primary measurements we chose to use a thermocouple technique in which radiation losses are compensated for by electrical heating of the thermocouple,[21] but because of this technique's complexity, we also used it to calibrate the radiation corrections of coated thermocouples which were not electrically heated. As a check, these radiation corrections were also calculated by the usual techniques. Fine wire S-type and B-type thermocouples 1 to 2 cm long with diameters from 50 to 125 μm were fused onto 250 μm wires of the same materials as saddle supports. The support wires fed through an alumina tube which was in turn inserted into a stainless steel 0.64 cm i.d. tube, vacuum-sealed with epoxy cement, and brought through the low pressure burner housing wall through a sliding O-ring seal.

In nonsooting flames catalytic heating of the thermocouple was avoided by coating the thermocouple with BeO/Y_2O_3.[22] The coating was fused at about 1870 K in a Meeker flame. In sooting flames the soot which rapidly formed on the probe was found to be a good noncatalytic coating. In some cases the thermocouple was intentionally soot-coated in a rich flame and rapidly used in a nonsooting flame before the coating burned off. The diameters of coated wires were measured before and after the experiments using a microscope to determine the coating thickness which was typically about 10-15 μm.

In the electrically heated thermocouple method, the thermocouple temperature is measured in a vacuum ($\leq 3 \times 10^{-3}$ Pa) as a function of heating current. This is done by resistively heating the wire with a 3 kHz a.c. current and simultaneously measuring the d.c. thermal emf of the thermocouple junction. In a good vacuum the convection losses are small or negligible so that the electrical power loss in the wire is equal to the radiation losses. A plot of junction temperature vs. heating current is thus generated. The experiment is then repeated in the flame producing another (different) plot of thermocouple temperature vs. heating current. If the two curves (one obtained in vacuum and one in the flame) are plotted on the same coordinate system they will cross at some point. If the radiative properties of the thermocouple (ϵ and d_w, where ϵ = the wire emissivity and d_w = the thermocouple wire diameter) do not change between the two experiments, the temperature at the crossing point is the true flame temperature. At this point there are no net losses from the thermocouple. To assure that the radiation properties of the thermocouple do not change during each experiment, the temperature-current curve is repeated in vacuum after each flame experiment .

The above procedure is tedious, and due to the fragile nature of the wire coating it was necessary to produce heating curves rapidly before the surface properties changed. Many thermocouples were lost, especially at the highest temperatures so that extrapolation procedures were developed.

Under vacuum conditions, in the absence of convection and conduction losses at the thermocouple junction, the energy balance involves only electrical heating and radiative losses to the surroundings. Equating the rates per unit wire length:

$$\sigma \epsilon \pi d_T \, (T_w^4 - T_s^4) = \frac{4\rho}{\pi d_w^2} I^2$$

where σ is the Stefan-Boltzmann constant, d_T is the total wire plus coating diameter, d_w is the diameter of the wire itself, ρ is the resistivity of the junction area and I is the heating current. The wire temperature, T_w, is much greater than the temperature of the surroundings, T_s so that

$$\sigma \epsilon \pi d_T \, T_w^4 = \frac{4\rho}{\pi d_w^2} I^2$$

The current required to heat the thermocouple to a temperature T_w is then:

$$I \propto d_w \left(\frac{d_T \epsilon}{\rho} \right)^{0.5} T_w^2$$

For platinum and rhodium alloys, both ϵ and ρ show similar temperature dependencies in the range of interest, 1000-2000 K. Therefore the overall current to temperature proportionality is $I \propto T_w^2$.

The calculated slopes dI/dT^2 should provide a measure of $(\epsilon d_T)^{0.5}$. The experimental values were grouped by the thermocouple visual appearance and dI/dT^2 normalized (to a new, shiny thermocouple). Slopes are given here:

Appearance	$(dI/dT_w^2)/(dI/dT_w^2)_{SHINY}$
Bare, shiny	1.00
Bare, not shiny	1.43
Bare, rough	1.57 ± 0.08
Dark coating, smooth - same diameter	1.80 ± 0.10
Dark coating, rough - same diameter	1.86 ± 0.05
Clean BeO/Y_2O_3 - thick	1.96
Dark BeO/Y_2O_3 - thick	2.36

This provides a rationale for extrapolation of the vacuum heating curves. Over 20 heating curves in vacuum were made for variously treated thermocouples. The current required to heat the thermocouples to any fixed temperature varied by nearly a factor of three, yet a linear least squares fit of T_w^2 vs. I, always gave a correlation coefficient $r^2 > 0.99$. The T_w^2 vs. I fitting routine was thus used to extrapolate to temperatures not directly accessible. The heating curves in the flame environment do not lend themselves to such simple closed form analysis since the convective heat transfer to the wire has a different temperature dependence from the radiation.

Three sets of heating curves are shown in Fig. 2 for two different thermocouples (circles and triangles) in a $\emptyset = 2.25$ flame, 21 mm above the burner and for one thermocouple (squares) 1.5 mm above the burner in the same flame. Thermocouple A was more heavily coated with carbon or soot for these measurements. Both thermocouples were B-type using 51 μm wires. The open symbols represent the vacuum calibration data while the solid symbols represent the heating curves in the flame. The curves through the open symbols are (linear) least squares fits to the data above 1000 K to the form: $I = a + bT_w^2$. (The line through the open circles represents a linear extrapolation of the four data points above 1300 K.) Either extrapolation method gives about the same result at the intersection of the vacuum and flame heating curves. The flame data (solid symbols) exhibit curvature at low currents. However, as the wire temperature increases, the T^4 heat loss term becomes more important and the

curvature decreases. Simulated heating curves calculated here have shown that the approach to the flame temperature is well approximated by a linear temperature vs. a.c. current relationship. We feel that a linear extrapolation of the flame data is more realistic, although it is recognized that uncertainties in extended extrapolation can be fairly large. Figure 2 supports the extrapolation method. The two thermocouples used at 21 mm have significantly different heating curves, yet the extrapolated flame temperatures are the same for both cases.

For thermocouples which are not electrically heated (I = 0), in the absence of catalytic heating and wire conduction losses (negligible with the long (~ 1 cm) fine wires used here), the heat balance equation gives the temperature correction for radiation for cylindrical thermocouples,

$$\Delta T \equiv T_{fl} - T_w \approx \frac{\sigma \epsilon}{h} T_w^4$$

where T_{fl} is the true local flame temperature, T_w is the thermocouple junction temperature, and h is the heat transfer coefficient from the flame gases to the wire. The temperature of the surroundings to which the thermocouple radiates is assumed to be small relative to T_w. The difference between the flame temperature from the intersection of the heating curves and the thermocouple reading with no heating current is the radiation correction, ΔT. The parameter h can be expressed as

$$h = \frac{k_f \, Nu}{d_T}$$

where k_f is the thermal conductivity of the flame gases and Nu is the Nusselt number. Thus,

$$\Delta T = \frac{\epsilon d_T \sigma T_w^4}{k_f \, Nu}$$

Under conditions appropriate to low Reynolds number, Re, as in these measurements, Nu has been approximated as[23] $0.8(Re)^{0.25}$ and as[24] $(0.42\ Pr^{0.2} + 0.57\ Pr^{0.33}\ Re^{0.5})$ where the Prandtl number Pr is roughly unity. In either case, Nu is only mildly dependent on the thermocouple dimensions ($Re \propto d_T$).

Thus, for the same position in a flame we estimate that the thermocouple response, in terms of $\Delta T/T_w^4$, is proportional to $(d_T \epsilon)$. The vacuum heating curves were shown above to scale as $I \propto (d_T \epsilon)^{0.5} T_w^2$. Therefore the radiation correction should be closely related to the square, $(dI/dT^2)^2$. For the two thermocouples used at 21 mm (Fig. 2) the ratio of the correction term $\Delta T/T_w^4$ is about 0.7 while the ratio of $(dI/dT_w^2)^2$ for the vacuum calibrations is about 0.6, consistent with the predictions.

In addition to the above procedures the heat transfer coefficient was calculated based on Kaskan's treatment[23] which assumes $Nu = 0.8(Re)^{0.25}$. Estimates of the flame composition were obtained from equilibrium calculations. Viscosity was calculated with Wilkes mixture rule and thermal conductivity was calculated with Wissiljewa's mixture rule as described in Ref. 25. For the three calibrations in Fig. 2 the experimental values of ΔT and the calculated values for h were consistent with a reasonable emissivity, $\epsilon = 0.8$. Due to uncertainties in the values of h, we do not claim to have measured ϵ but an elevated emissivity above that for a shiny thermocouple is consistent both with visual observations of carbonaceous coatings formation in these nonsooting flames and with the vacuum calibrations.

Determination of flame temperatures with thermocouple heating curves is both time consuming and tedious. However, one can make use of any single measurement to determine ϵ/h for a thermocouple in a particular flame as described above. Since

$$\frac{\epsilon}{h} = \frac{\epsilon d_T}{k_f \, Nu}$$

one can estimate the variation in ϵ/h and thence the radiation correction, ΔT. The Nusselt number is assumed to only weakly depend on the local flame properties. For a given thermocouple with a fixed surface, ϵd_T is constant. Note that dI/dT_w^2 is a measure of this for any specific thermocouple and can be used to check the thermocouple properties. The thermal conductivity k_f is composition and temperature dependent. However, the major product gases in $\phi = 2.5$ to 3.5 flames have similar thermal conductivities, so the calculated temperature dependence of k_f of about T^1 is the major correction factor. Electrically heated thermocouple temperature measurements were made near the location of the maximum temperature, at T_{max}, in the $\phi = 3.0$ flame (at 1.0 cm from burner). The values of 1883 and 1923 K were determined with two different thermocouples. The differences between the uncorrected thermocouple reading in the flame and the flame temperature was on the order of 270-300 K. Two values of ϵ/h were then calculated and the mean value was used to correct all the flame profiles for $2.5 \leq \phi \leq 3.5$, correcting for the temperature dependence of k_f scaled as T^1. With correction factors on the order of 200 to 400 K, the inclusion of temperature dependent k_f normally changed the correction by less than 40 K. The effect of flame composition variations was assumed to be negligible although this is not a good approximation in the region between the burner and the temperature maximum. However, in this region corrections tend to be lower and limited spatial resolution introduces comparable uncertainties. For example, at 4 mm in a $\phi = 3.0$ flame, the temperature gradient is about 100 K/mm and the estimated thermocouple correction factor is 200 K. A 50% change in the thermal conductivity would cause an error in the corrected temperature only to the spatial resolution of the thermocouple. Because the calculated ion concentrations derived from Langmuir probe data are not greatly affected by errors of this magnitude, we do not attempt more complicated corrections close to the burner.

Measurements were also made in $\emptyset$ = 2.25 flames using the electrical heating technique. As previously shown (Fig. 2) a heavily sooted thermocouple (A) and the lightly sooted thermocouple (B) measurement at 21 mm from the burner gave the same temperature even though radiative properties (vacuum calibrations) differed considerably. The value of ϵ/h extracted for the lightly sooted wire (thermocouple B) was used to correct the temperatures in two rapidly recorded unheated thermocouple profiles as described above. The agreement in the region of overlap was about ± 20 K. Other heating curve measurements of the temperatures nearer the burner, while somewhat uncertain, are in accord with these profiles.

Temperature profiles in leaner flames (e.g., $\emptyset$ = 1.5, 1.75, 2.00) are complicated by catalytic heating. Use of either a heavy BeO/Y_2O_3 coating of 10 to 20 μm thickness or a soot coating (10 μm thickness) eliminated this effect. Both thermocouples had similar dI/dT^2 ($\propto (\epsilon d_T)^{0.5}$) values measured in a vacuum. The assumption of equal values of ϵ/h for the two thermocouples gave about 30-40 K difference between the two experimental temperature profiles in any flame.

Overall, the maximum difference in temperature measured at any point in any flame is about ± 60 K (± 80 K in $\emptyset$ = 2.0) while typically any difference near and downstream of T_{max} is closer to ± 30 K (± 40 K in $\emptyset$ = 2.0).

Temperature measurements in several flames of interest were made by the above technique and are reported in Figs. 3 and 4. Figure 3 gives profiles on the AeroChem stainless steel burner at several equivalence ratios, $\emptyset$. The flames are all acetylene-oxygen (p = 2.7 kPa, unburned gas velocity u = 50 cm/s). In Fig. 4 the temperature profile on the AeroChem stainless steel burner and on the MIT copper burner are compared for a $\emptyset$ = 3.0 flame. In obtaining these data three different thermocouple wire diameters were used, 51, 76, and 127 μm. The range in temperature among them was ~ ± 2%. The temperature differences between the two burners, Fig. 4, are certainly due to differences in thermal losses, mostly to the cooled burner surface. The calculated adiabatic flame temperature for these conditions is 2772 K. The temperature profiles decrease with different slopes, e.g., the MIT burner flame temperature decreases more rapidly than does the temperature on the AeroChem stainless steel burner. When the temperature profiles reported here and by others[14,26] are plotted against the distance above the burner divided by the burner diameter, the temperature profiles become parallel, Fig. 5.

C. ABSOLUTE ION CONCENTRATIONS IN SOOTING FLAMES

Using the temperature profiles determined as above, absolute ion concentrations were determined with the Langmuir probe technique developed under the previous contract[27] and refined here. These results were reported at the Twentieth Combustion Symposium[5] and will not be discussed here in detail. The major points in that paper were: (1). The absolute ion concentration in the "standard flame" (acetylene-oxygen, $\emptyset$ = 3.0, p = 2.7 kPa, u = 50 cm/s) Fig. 6,

can now be accepted; AeroChem's probe results and Homann's ion molecular beam sampling agree--previously ion concentration measurements reported in this flame varied by several orders of magnitude.[28] (2). The concentration of ions preceding the appearance of soot and the decay of ions are consistent with the ionic mechanism of soot formation, see Fig. 6. Absolute ion concentration profiles have been determined for a number of other equivalence ratios in similar flames (p = 2.7 kPa, u = 50 cm/s) and some are given in Fig. 7. (3). One of the major arguments which had been quoted by Delfau et al.[13] and Haynes and Wagner[29] against the ionic mechanism of soot formation--namely that as the equivalence ratio of a flame is increased the ion concentration seems to increase at just the equivalence ratio at which soot is formed, Fig. 8--was demonstrated to be invalid experimentally. In addition to other arguments, there are actually two ion peaks involved, and the second peak occurs too far ahead of the formation of soot to be derived from the soot.

D. CHARACTERISTIC REACTION TIMES

The availability of reliable temperature and total ion concentration data makes it possible to interpret the flame reactions in terms of characteristic times; this is useful in determining the importance of the various individual processes and is thus a first step to modeling the overall process because the key processes can be identified. We report in Figs. 9 and 10 the characteristic times for the flame in Fig. 6 at locations 1.5 and 2.5 cm above the burner. The times are to be compared with the experimental flow time; processes occurring at the longer characteristic times are less important and the shorter characteristic times are most important. Some of the steps need occur only once so the times are directly comparable: other steps must occur as many as 10^3 times by the time the flow reaches 2.5 cm. These individual steps must therefore be very rapid, i.e., less than 10^{-6} s per step. The rate coefficients used for this analysis are those quoted by the protagonist of the reaction. The value of k_c is either the hard sphere collision cross-section for R (R is a hydrocarbon) assumed to be a six-carbon ring compound, or the Langevin cross-section for an ion R^+ (including $C_3H_3^+$ and very large ions). P, P^+, and P^- represent soot particles of the size observed at 2.5 cm above the burner in this flame.

One observation which emerges from the present exercise is that, for low molecular weights, ion-molecule reactions are distinctly faster than neutral-neutral reactions; however, an increase in molecular size (assuming C_2H_2 as the building block), and an increase in temperature both favor neutral-neutral reactions. Also, as ions increase in size, their recombination coefficients increase, so that the larger ions are removed more rapidly than the smaller ions. Thus, as the incipient soot particles grow, the ionic nature of the process becomes less important. This explains one of the mysterious observations that neutral soot particles appear to grow more rapidly than do charged particles (see, e.g., Fig. 4, Ref. 2).

E. TEMPERATURE EFFECTS

Some measurements of the effect of temperature on soot formation in premixed flames were made with very surprising results. This work has been pubished[30] and so it will be only cursorily summarized here with a brief discussion of some of the implications which we have not yet explored. In these experiments soot formation was observed in atmospheric pressure toluene and decalin flames of various fuel/O_2/N_2 mixtures. As the $O_2/(O_2 + N_2)$ ratio was increased, the onset of sooting occurred at higher fuel/O_2 ratios, and at higher calculated flame temperatures, consistent with previous observations of others.[31,32] However, when the temperatures were measured using two-wavelength emission pyrometry, the flame temperatures at the soot thresholds were constant for each fuel (1750 K for toluene and 1720 K for decalin). These results for toluene are displayed in Fig. 11. Soot volume fractions, f_v were also measured under a Naval Research Laboratory contract,[33] using a multiwavelength laser extinction technique, as a function of equivalence ratio, $O_2/O_2 + N_2$ ratio, and the experimental flame temperature. The soot volume fractions varied strongly with the $O_2/(O_2 + N_2)$ ratio, but the variation with measured temperature was independent of the $O_2/(O_2 + N_2)$ ratio. It, in fact, appeared in these experiments that the soot yield, for each fuel, at and above soot threshold was uniquely determined by the measured flame temperature, independent of how this temperature was obtained.

These results clearly indicate the hazards involved in using adiabatic flame temperatures instead of measured temperatures in interpreting soot formation studies. The results in Fig. 11 imply that, as the equivalence ratio is increased, some of the heat release reactions do not go to completion- - other obvious explanations can be rejected.[30]

Probably related to the above is the equilibrium or nonequilibrium nature of soot formation in flames. It is generally accepted that at the threshold for soot formation the production of soot is not predicted by an adiabatic equilibrium calculation but that soot formation requires a nonequilibrium mechanism for its formation. We, in fact, use this as an argument for the ionic mechanism of soot formation which depends upon the nonequilibrium formation of chemi-ions to drive the process. We have, however, made some equilibrium calculations of the quantity of soot formed in flames at fuel concentrations exceeding the threshold fuel composition, and they seem to predict an excess of soot over that measured. This work needs further evaluation and substantiation before we are willing to report it publicly; if substantiated it would mean a completely different mechanism might be involved in flames near soot threshold and in very rich mixtures!

F. EQUIVALENCE RATIOS

It has been customary in the combustion community to express the composition of a fuel-oxidizer mixture as an equivalence ratio calculated by assuming the products are H_2O and CO_2. The equivalence ratio is then defined as:

$$\phi = \frac{(\text{Fuel/Oxidizer})_{ACTUAL}}{(\text{Fuel/Oxidizer})_{CALCULATED}}$$

While this is usually satisfactory it has been recognized to be somewhat misleading for fuel rich mixtures, such as encountered in soot work. Some people use the C/O ratio[16,29] and some have chosen to assume the product is CO rather than CO_2.[34] In search of some guidance on how to treat this problem we have calculated the adiabatic equilibrium composition at the soot threshold for a set of fuels spanning the threshold soot index, TSI, range from 0 to 100[35,36]; the results are plotted in Fig. 12. It is clear that CO is no better choice than CO_2 and that H_2O is similarly a poor choice.

The linear variations of the ratios plotted in Fig. 12 are interesting but their significance is not clear; they are probably an important consideration in the equilibrium/nonequilibrium problem poised above!

III. PUBLICATIONS

The following paper was published during this report period:

1. "Ion Concentrations in Premixed Acetylene-Oxygen Flames Near the Soot Threshold," Keil, D.G., Gill, R.J., Olson, D.B., and Calcote, H.F., in The Chemistry of Combustion Processes, T.M. Sloane, Ed., ACS Symposium Series 249 (American Chemical Society, Washington, DC, 1984) pp. 33-47

The following papers were submitted for publication during this period:

1. "Ionization and Soot Formation in Premixed Flames," Keil, D.G., Gill, R.J., Olson, D.B., and Calcote, H.F., Twentieth Symposium (International) on Combustion (in press).

2. "The Effect of Temperature on Soot Formation in Premixed Flames," Olson, D.B. and Madronich, S., AeroChem TP-446, submitted to Combust. Flame, August 1984.

The following manuscript is in preparation:

1. "Langmuir Probe Measurements in Sooting Flames," Keil, D.G., Gill, R.J., Olson, D.B., and Calcote, H.F.

IV. PERSONNEL

In addition to the authors the following personnel made significant contributions to this program:

Douglas B. Olson, Physical Chemist
Robert J. Gill, Physical Chemist
John C. Pickens, Technician
Helen Rothschild, Librarian and Technical Editor
Evangeline Stokes, Technical Typist

V. TECHNICAL INTERACTIONS

Technical interactions with other members of the scientific community have taken several forms, the foremost being presentation of our work at scientific meetings, seminars, and workshops. Proposals and manuscript reviews, an important interaction, require an increasing effort. Personal contacts with other technical people in this field have been maintained by attending meetings, and by correspondence and phone calls.

The following presentations were made during this reporting period or were not previously reported:

1. "Soot Formation in Combustion," H.F. Calcote, Seminar, Stevens Institute of Technology, Hoboken, NJ, 9 February 1983.

2. "Ion Concentrations in Premixed Acetylene Flames," D.G. Keil, R.J. Gill, and D.B. Olson, Chemistry of Combustion Processes Symposium, 185th National Meeting, American Chemical Society, Seattle, WA, 20-25 March 1983.

3. "Ionic Mechanisms of Soot Formation in Flames," H.F. Calcote and D.B. Olson, AFOSR Contractors Meeting on Airbreathing Combustion Dynamics Research, Scottsdale, AZ, 19-23 September 1983.

4. "Use of Langmuir Probes in Low Pressure Sooting Flames," D.G. Keil and R.J. Gill, Fall Technical Meeting, Eastern Section: The Combustion Institute, Providence, RI, 8-10 November 1983.

5. "Ionic Structure of Sooting Flames," H.F. Calcote, R.J. Gill, D.G. Keil, and D.B. Olson, Fall Technical Meeting, Eastern Section: The Combustion Institute, Providence, RI, 8-10 November 1983.

6. "An Ionic Mechanism of Soot Formation in Flames," H.F. Calcote, Invited Presentation, American Physical Society Meeting, Detroit, MI, 26-30 March 1984.

7. "Ionic Mechanism of Soot Formation - Toward a Quantitative Model," H.F. Calcote, NBS Workshop on Flame Radiation and Soot, Gaithersburg, MD, 10 May 1984.

8. "Ionic Mechanisms of Soot Formation in Flames," H.F. Calcote, AFOSR/ONR Contractors Meeting in Combustion, Carnegie-Mellon University, Pittsburgh, PA, 20-21 June 1984.

9. "The Effect of Temperature on Soot Formation in Premixed Flames," D.B. Olson and S. Madronich, AeroChem Soot Workshop, Princeton, NJ, 13 July 1984.

10. "Ionic Theory of Soot Formation," H.F.Calcote, AeroChem Soot Workshop, Princeton, NJ 13 July 1984.

11. "Ionization and Soot Formation in Premixed Flames," D.G. Keil, R.J. Gill, D.B. Olson, and H.F. Calcote, Twentieth Symposium (International) on Combustion, University of Michigan, Ann Arbor, MI, 12-17 August 1984.

VI. INVENTIONS AND PATENT DISCLOSURES

There were no inventions or patent disclosures to report during this period.

VII. REFERENCES

1. Calcote, H.F., "Ionic Mechanism of Soot Formation," in Soot in Combustion Systems and Its Toxic Properties, J. Lahaye and G. Prado, Eds. (Plenum Press, New York, 1983) p. 197.

2. Calcote, H.F. "Mechanism of Soot Nucleation in Flames - A Critical Review," Combust. Flame 42, 215 (1981).

3. Olson, D.B. and Calcote, H.F., "Ionic Mechanism of Soot Nucleation in Premixed Flames," in Particulate Carbon: Formation During Combustion, D.C. Siegla and G.W. Smith, Eds. (Plenum Press, New York, 1981) p. 177.

4. Olson, D.B. and Calcote, H.F., "Ions in Fuel-Rich and Sooting Acetylene and Benzene Flames," Eighteenth Symposium (International) on Combustion (The Combustion Institute, Pittsburgh, 1981) p. 453.

5. Keil, D.G., Gill, R.J., Olson, D.B. and Calcote, H.F., "Ionization and Soot Formation in Premixed Flames," Twentieth Symposium (International) on Combustion (The Combustion Institute, Pittsburgh, 1985) p. 1129.

6. Smoot, L.D. and Hill, S.C., "Critical Requirements in Combustion Research," Prog. Energy Combust. Sci. 9, 77 (1983).

7. Palmer, H.B. and Cullis, C.F., "The Formation of Carbon from Soot," in Chemistry and Physics of Carbon, Vol. I, P.L. Walker, Jr., Ed. (Marcel Dekker, New York, 1965) p. 265.

8. Frenklach, M, Clary, D.W., Gardiner, W.C., Jr., and Stein, S.E.,"Detailed Kinetic Modeling of Soot Formation in Shock-Tube Pyrolysis of Acetylene," Twentieth Symposium (International) on Combustion (The Combustion Institute, Pittsburgh, 1985) p. 887.

9. Howard, J.B., Wersborg, B.L., and Williams, G.C., "Coagulation of Carbon Particles in Premixed Flames," Faraday Soc. Symp. 7, 109 (1973).

10. Wersborg, B.L., Yeung, A.C., and Howard, J.B., "Concentration and Mass Distribution of Charged Species in Sooting Flames," Fifteenth Symposium (International) on Combustion (The Combustion Institute, Pittsburgh, 1975) p. 1439.

11. Bittner, J.D. and Howard, J.B., "Pre-Particle Chemistry in Soot Formation," in Particulate Carbon: Formation During Combustion, D.C. Siegla and G.W. Smith, Eds. (Plenum Press, New York, 1981) p. 109.

12. Michaud, P., Delfau, J.L., and Barassin, A., "The Positive Ion Chemistry in the Post-Combustion Zone of Sooting Premixed Acetylene Low Pressure Flat Flames," Eighteenth Symposium (International) on Combustion (The Combustion Institute, Pittsburgh, 1981) p. 443.

13. Delfau, J.L., Michaud, P., and Barassin, A., "Formation of Small and Large Positive Ions in Rich and Sooting Low-Pressure Ethylene and Acetylene Premixed Flames," Combust. Sci. Tech. 20, 165 (1979).

14. Delfau, J.L. and Vovelle, C., "Mechanism of Soot Formation in Premixed C_2H_2/O_2 Flames," Combust. Sci. Tech. 41, 1 (1984).

15. Homann, K.H., "Formation of Large Molecules, Particulates and Ions in Premixed Hydrocarbon Flames; Progress and Unresolved Questions," Twentieth Symposium (International) on Combustion (The Combustion Institute, Pittsburgh, 1985) p. 857.

16. Homann, K.H., "Charged Particles in Sooting Flames I. Determination of Mass Distributions and Number Densities in C_2H_2-O_2 Flames," Ber. Bunsenges. Phys. Chem. 83, 738 (1979).

17. Homann, K.H., Strofer, E., and Wolf, H., "Growth of Electrically Charged Soot Particles in Flames," Combustion Problems in Turbine Engines, AGARD Conference Proceedings No. 353, January 1984, p. 19-1. (1984).

18. Homann, K.H. and Schweinfurth, H., "Kinetics and Mechanism of Hydrocarbon Formation in the System C_2H_2/O/H," Ber. Bunsenges. Phys. Chem. 85, 569 (1981).

19. Howard, J.B., MIT, Personal communication.

20. Keil, D.G., Gill, R.J., Olson, D.B., and Calcote, H.F., "Ion Concentrations in Premixed Acetylene-Oxygen Flames Near the Soot Threshold," in The Chemistry of Combustion Processes, T.M. Sloane, Ed., ACS Symposium Series 249 (American Chemical Society, Washington, DC, 1984) p. 33.

21. Hayhurst, A.N. and Kittelson, D.B., "Heat and Mass Transfer Considerations in the Use of Electrically Heated Thermocouples of Iridium versus an Iridium/Rhodium Alloy in Atmospheric Pressure Flames," Combust. Flame 28, 301 (1977).

22. Kent, J.H., "A Noncatalytic Coating for Platinum-Rhodium Thermocouples," Combust. Flame 14, 279 (1970).

23. Kaskan, W.E., "The Dependence of Flame Temperature on Mass Burning Velocity," Sixth Symposium (International) on Combustion (Reinhold Publishing Corp., New York, 1957) p. 134.

24. Bradley, D. and Matthews, K.J., "Measurement of High Gas Temperatures with Fine Wire Thermocouples," J. Mech. Engn. Sci. 10, 299 (1968).

25. Reid, R.C. and Sherwood, T.K., The Properties of Gases and Liquids, 2nd ed. (McGraw-Hill, New York, 1966) Ch. 9 and 10.

26. Bonne, U. and Wagner, H.Gg., Ber. Bunsenges. Phys. Chem. 69, 35 (1965).

27. Calcote, H.F. and Olson, D.B., "Ionic Mechanisms of Soot Formation in Flames," Final Report, AeroChem TP-443, May 1984.

28. See discussion following Ref. 4.

29. Haynes, B.S. and Wagner, H.Gg., "Soot Formation," Progr. Energy Combust. Sci. 7, 229 (1981).

30. Olson, D.B. and Madronich, S., "The Effect of Temperature on Soot Formation in Premixed Flames," Combust. Flame 60, 203 (1985).

31. Street, J.C. and Thomas, A., "Soot Formation in Premixed Flames," Fuel 34, 4 (1955).

32. Millikan, R.C., "Non-equilibrium Soot Formation in Premixed Flames," J. Phys. Chem. 66, 784 (1962).

33. Naval Research Laboratory, Contract No. N00014-83-C-2311.

34. Takahashi, F. and Glassman, I., "Sooting Correlations for Premixed Flames," Combust. Sci. Tech. 37, 1 (1984).

35. Calcote, H.F. and Manos, D.M., "Effect of Molecular Structure on Incipient Soot Formation," Combust. Flame 49, 289 (1983).

36. Olson, D.B. and Pickens, J.C., "The Effects of Molecular Structure on Soot Formation, I. Soot Thresholds in Premixed Flames," Combust. Flame 57, 199 (1984).

FREE RADICAL MECHANISM

(Frenklach, Clary, Gardiner, and Stein)

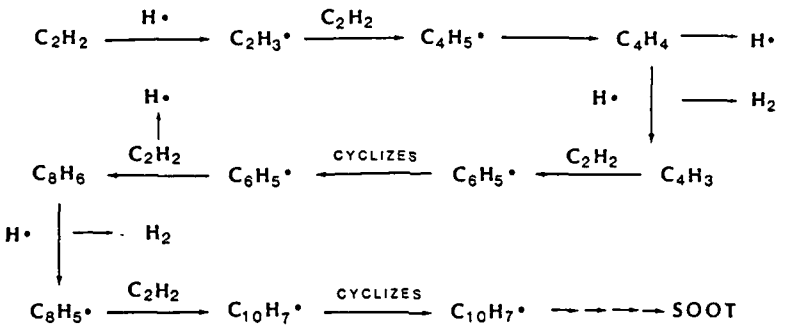

IONIC MECHANISM

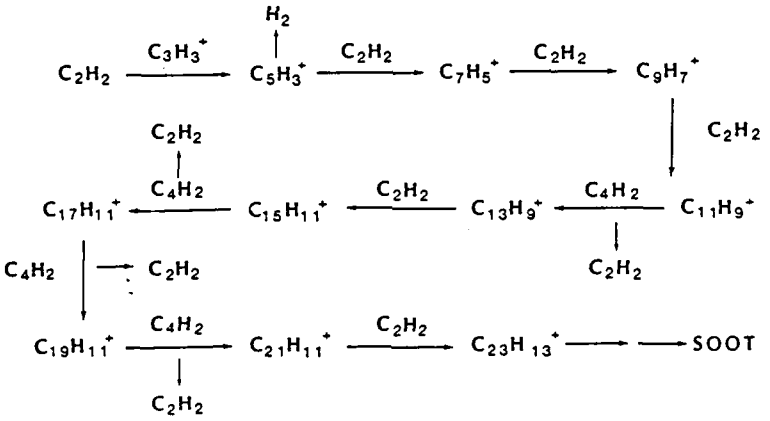

FIGURE 1 COMPARISON OF INITIAL STEPS IN FREE RADICAL[8] AND IONIC MECHANISMS OF SOOT FORMATION

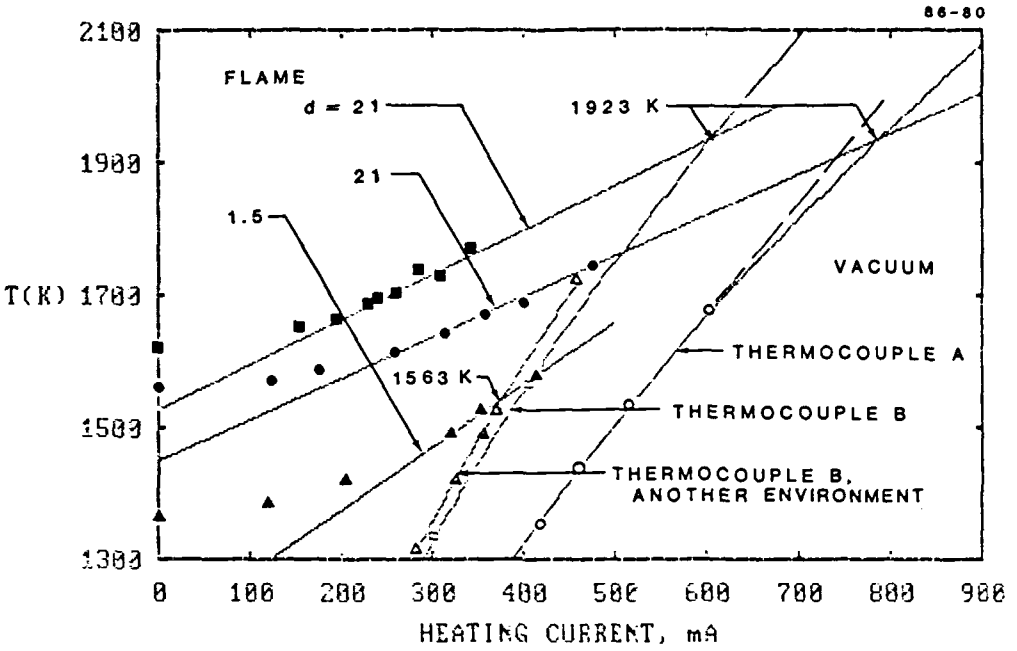

FIGURE 2 THERMOCOUPLE HEATING CURVES IN VACUUM (OPEN SYMBOLS) AND IN Ø = 2.25 FLAMES (CLOSED SYMBOLS)

Distances from the burner are given in mm. The intersections of matched solid curves (see text) give the indicated experimental flame temperatures. Dashed curve - linear extrapolation of thermocouple A vacuum data (see text).

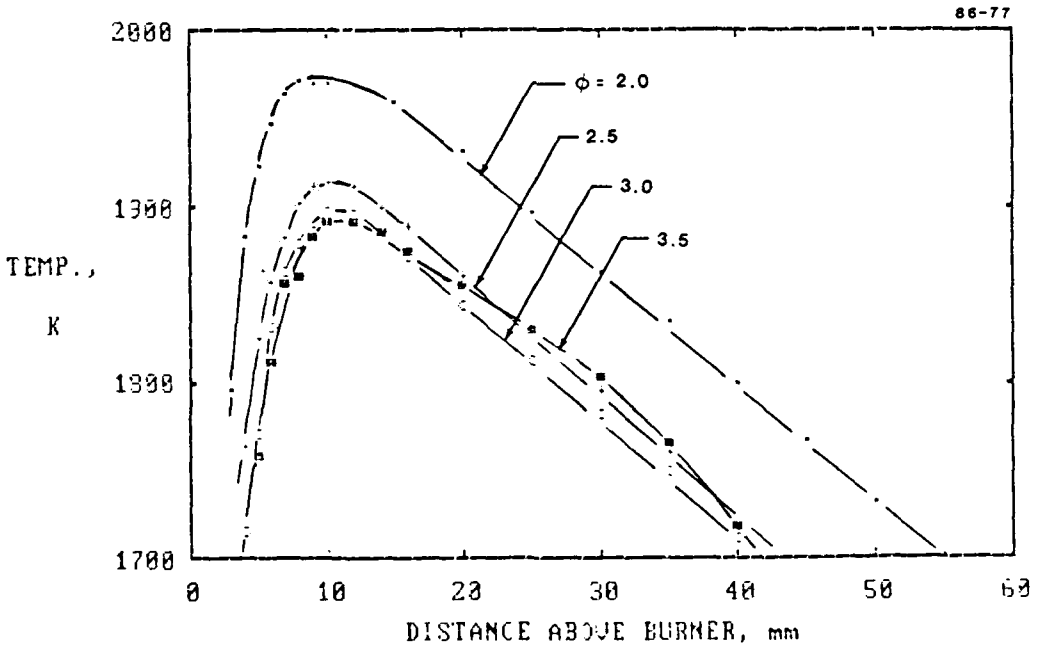

FIGURE 3 EXPERIMENTAL TEMPERATURE PROFILES FOR ACETYLENE-OXYGEN FLAMES FOR DIFFERENT EQUIVALENCE RATIOS

Stainless steel burner, low pressure flames (see text).

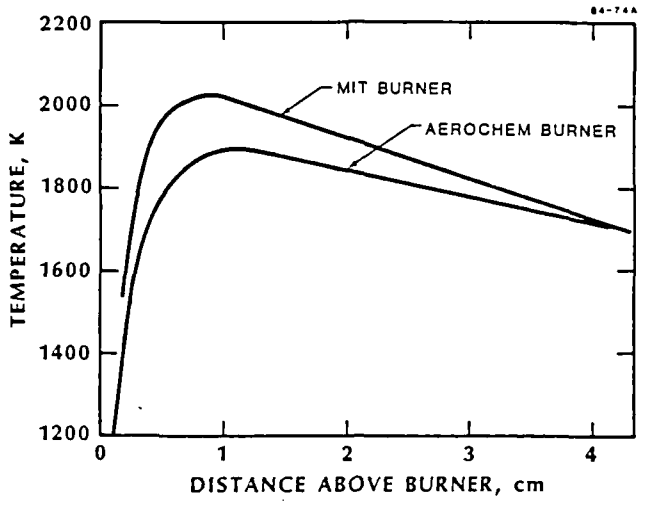

FIGURE 4 COMPARISON OF TEMPERATURE PROFILES IN THE MIT DESIGN COPPER BURNER AND THE AEROCHEM STAINLESS STEEL MULTITUBE BURNER

Ø = 3.0 flames (see text).

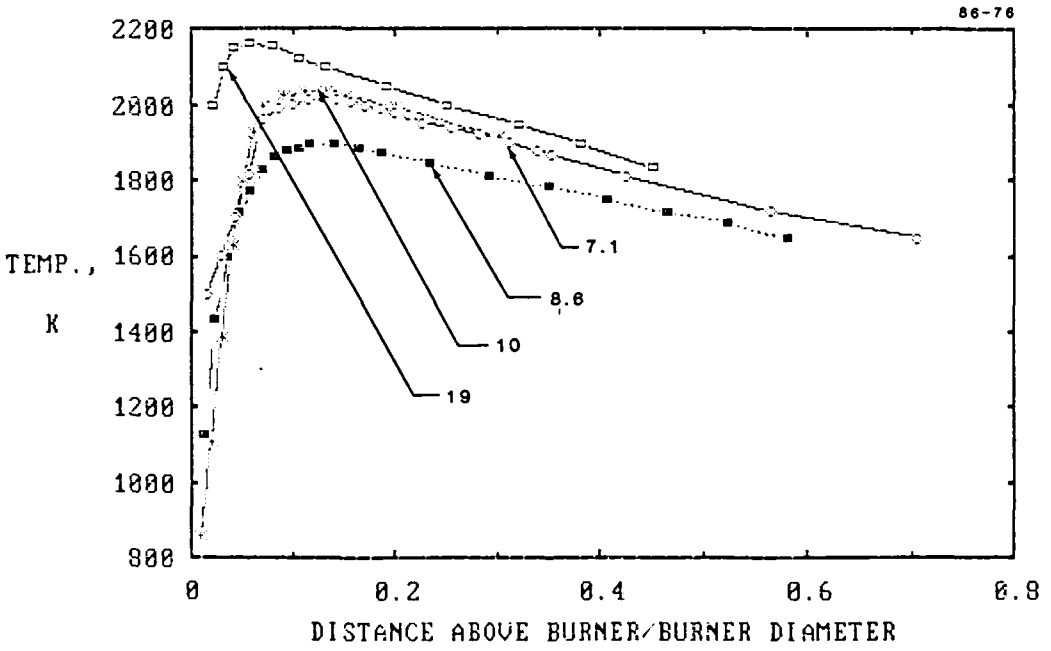

FIGURE 5 TEMPERATURE PROFILES AS FUNCTION OF DISTANCE ABOVE BURNER NORMALIZED BY BURNER DIAMETER

□ - Ref. 26, Ø = 3.5; * - Ref. 14 with diameter from Ref. 13 assumed; O - MIT design copper burner; ■ - AeroChem stainless steel burner. All acetylene-oxygen flames (p = 2.7 kPa, u = 50 cm/s). Ø = 3.0 unless noted otherwise. Diameters indicated in cm.

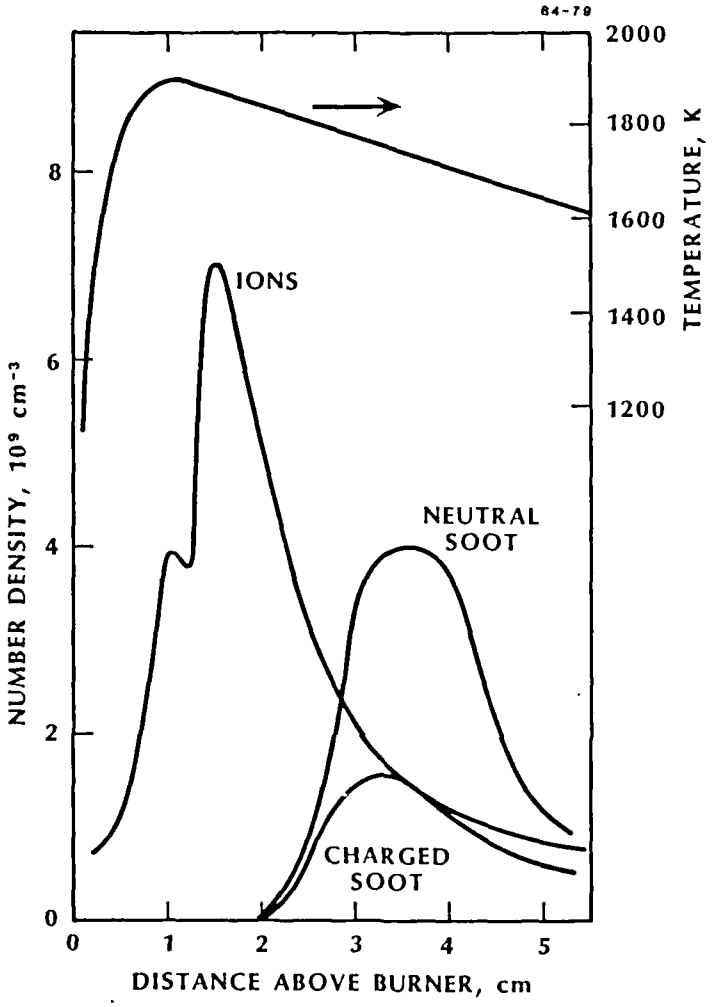

FIGURE 6 COMPARISON OF TOTAL ION CONCENTRATION WITH NEUTRAL AND CHARGED SOOT PARTICLES (d) 1.5 nm) FROM HOWARD ET AL.[9]

The particle concentrations have been reduced to agree with ions at 3.5 cm above the burner. Ø = 3.0. (See text.)

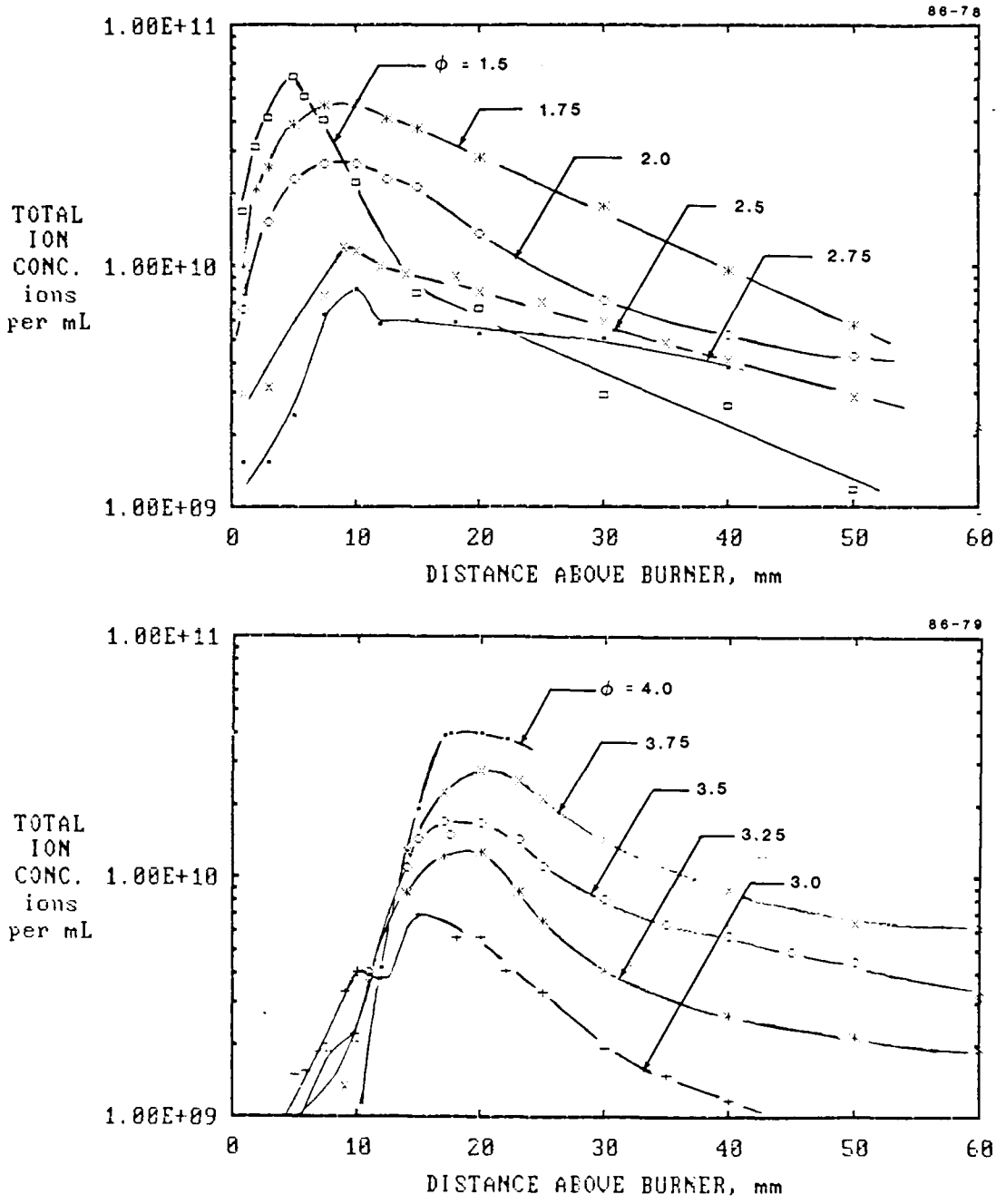

FIGURE 7 TOTAL ION CONCENTRATION PROFILES BY LANGMUIR PROBE TECHNIQUE FOR ACETYLENE-OXYGEN FLAMES ON STAINLESS STEEL BURNER

Curves are at indicated equivalence ratios. (See text.)

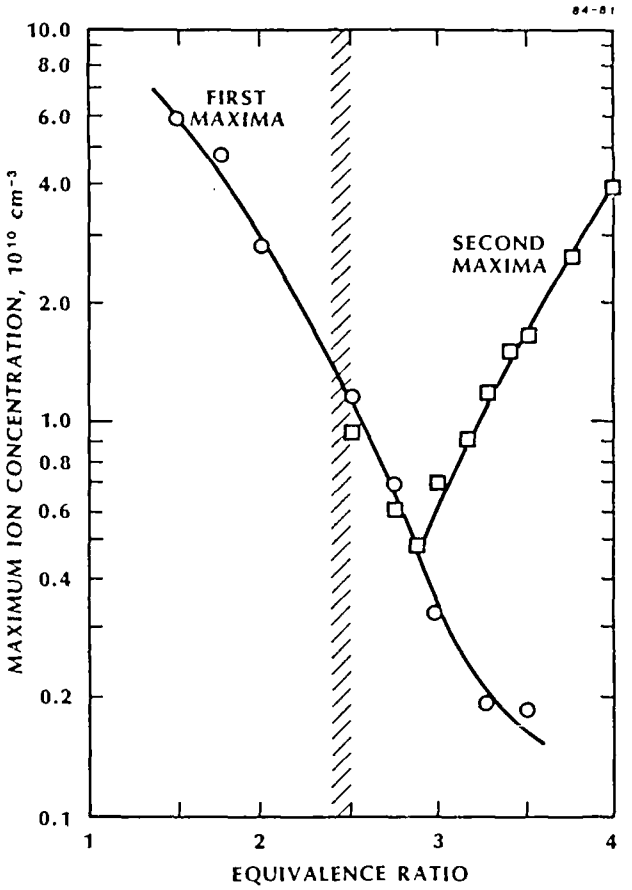

FIGURE 8 VARIATION OF MAXIMUM TOTAL ION CONCENTRATION WITH EQUIVALENCE RATIO

Acetylene-oxygen, p = 2.7 kPa, u = 50 cm/s

84-71

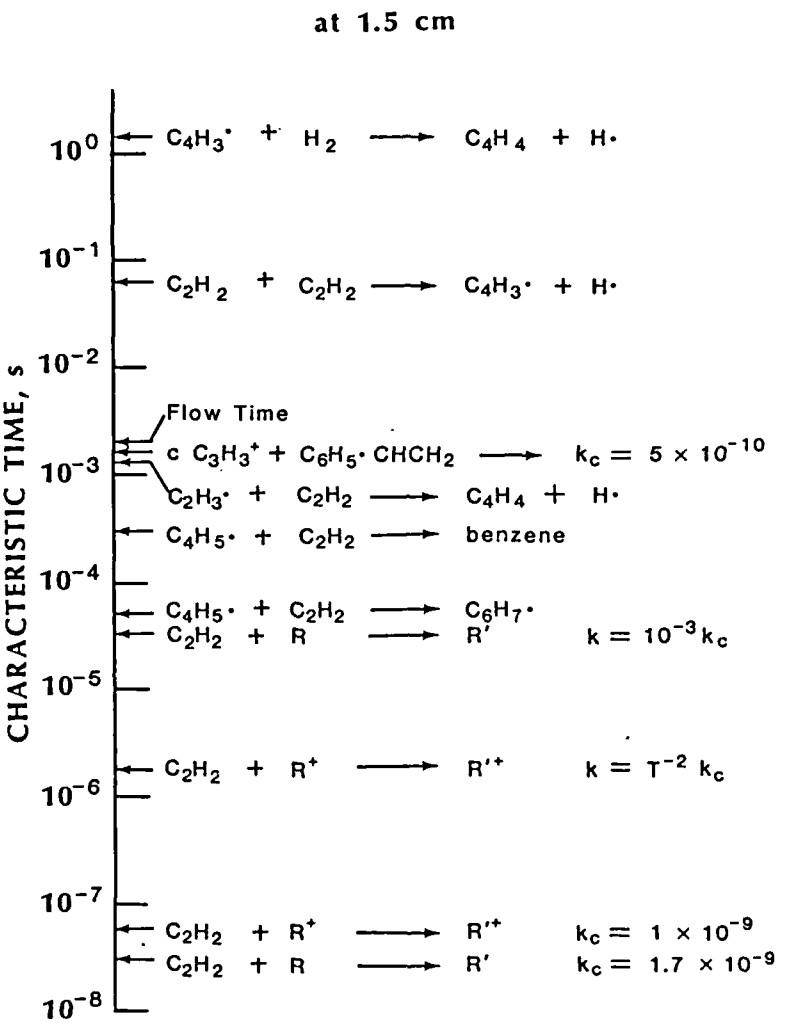

FIGURE 9 CHARACTERISTIC TIMES AT 1.5 cm ABOVE BURNER FOR FLAME IN FIGURE 6

84-70

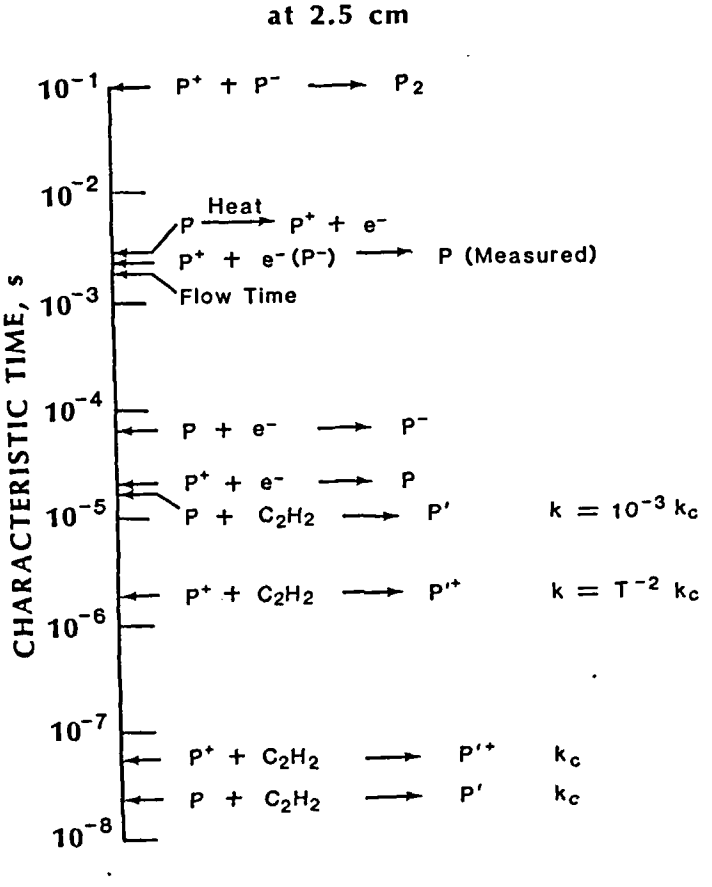

FIGURE 10 CHARACTERISTIC TIMES AT 2.5 cm ABOVE BURNER FOR FLAME IN FIGURE 6

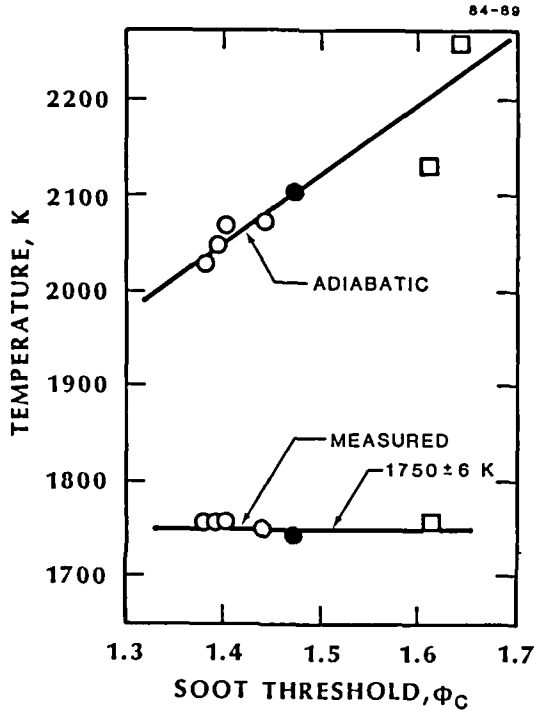

FIGURE 11 COMPARISON OF ADIABATIC AND MEASURED TEMPERATURES AS A FUNCTION OF SOOT THRESHOLD, ϕ_c, FOR ATMOSPHERIC TOLUENE/O_2/N_2 FLAMES

○ - $O_2/(O_2 + N_2)$ < 0.21; ● - Fuel-Air Mixtures
□ - $O_2/(O_2 + N_2)$ > 0.21.

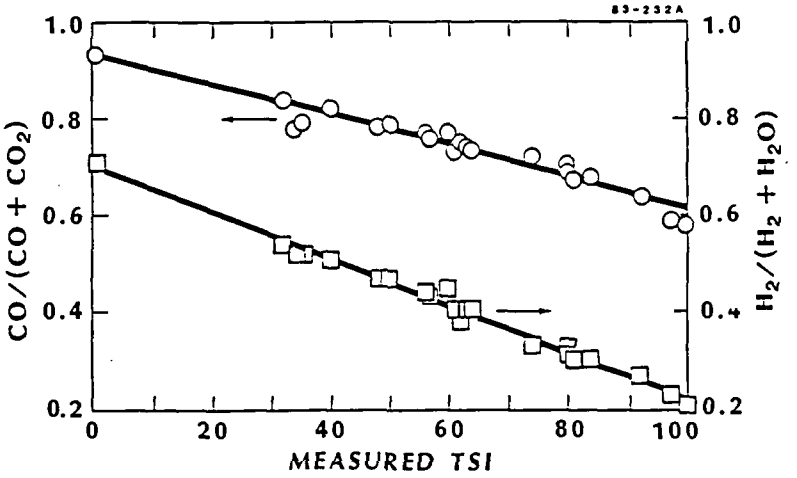

FIGURE 12 EQUILIBRIUM COMPOSITIONS CALCULATED AT THE MEASURED SOOT THRESHOLD FOR A SERIES OF FUELS

END

12-86

DTIC